Free Radical Biology & Medicine, Vol. 30, No. 8, pp. 825–835, 2001

0891-5849/01/$–see front matter

PII S0891-5849(01)00469-5

Original Contribution

PHOSPHOLIPID HYDROPEROXIDE GLUTATHIONE PEROXIDASE PROTECTS AGAINST SINGLET OXYGEN-INDUCED CELL DAMAGE OF PHOTODYNAMIC THERAPY

HONG P. WANG, STEVEN YUE QIAN, FREYA Q. SCHAFER, FREDERICK E. DOMANN, LARRY W. OBERLEY, and GARRY R. BUETTNER

Free Radical and Radiation Biology Program, Department of Radiology, College of Medicine, The University of Iowa, Iowa City, IA, USA

(*Received* 9 *November* 2000; *Revised* 9 *January* 2001; *Accepted* 9 *January* 2001)

Abstract—Phospholipid hydroperoxide glutathione peroxidase (PhGPx) is an important enzyme in the removal of lipid hydroperoxides (LOOHs) from cell membranes. Cancer treatments such as photodynamic therapy (PDT) induce lipid peroxidation in cells as a detrimental action. The photosensitizers used produce reactive oxygen species such as singlet oxygen ($^1O_2$). Because singlet oxygen introduces lipid hydroperoxides into cell membranes, we hypothesized that PhGPx would provide protection against the oxidative stress of singlet oxygen and therefore could interfere with cancer treatment. To test this hypothesis, human breast cancer cells (MCF-7) were stably transfected with PhGPx cDNA. Four clones with varying levels of PhGPx activity were isolated. The activities of other cellular antioxidant enzymes were not influenced by the overexpression of PhGPx. Cellular PhGPx activity had a remarkable inverse linear correlation to the removal of lipid hydroperoxides in living cells ($r = -0.85$), and correlated positively with cell survival after singlet oxygen exposure ($r = 0.94$). These data demonstrate that PhGPx provides significant protection against singlet oxygen-generated lipid peroxidation via removal of LOOH and suggest that LOOHs are major mediators in this cell injury process. Thus, PhGPx activity could contribute to the resistance of tumor cells to PDT. © 2001 Elsevier Science Inc.

Keywords—Lipid peroxidation, Free radicals, EPR, PDT, PhGPx

INTRODUCTION

Lipid hydroperoxides (LOOHs) are key detrimental species involved in the mechanism of some current treatments of cancer, such as photodynamic therapy (PDT). The peroxidation of membrane lipids is a major consequence of oxidative stress. The oxidation of lipids, particularly phospholipids, has also been suggested to be a significant chemical event in a variety of pathological conditions, such as atherosclerosis, ischemic injury, and carcinogenesis [1–3]. The formation of lipid hydroperoxides (LOOHs) within the bilayer of membranes disrupts membrane structure and function [4], which subsequently leads to cell injury and death.

The repair of intracellular LOOHs can be carried out by cytosolic glutathione peroxidase (cGPx) [5], phospholipid hydroperoxide glutathione peroxidase (PhGPx) [6], nonselenium GPx [7], or glutathione-S-transferase (GST) [8]. However, cGPx requires the cooperative action of phospholipase A_2 (PLA_2) for the removal of LOOHs [8]. PhGPx is able to directly reduce both phospholipid- and cholesterol-hydroperoxides in cell membranes [6,9] (see Reactions 1–4). The rate of removal of LOOHs by PhGPx has been estimated to be about four orders of magnitude higher than the rate of removal by cGPx and PLA_2 [10].

$$\mathrm{LOOH + H^+ + PhGPx\text{-}Se^- \rightarrow LOH + PhGPx\text{-}SeOH} \quad (1)$$

$$\mathrm{PhGPx\text{-}SeOH + GSH \rightarrow PhGPx\text{-}Se\text{-}SG + H_2O} \quad (2)$$

$$\mathrm{PhGPx\text{-}Se\text{-}SG + GSH \rightarrow PhGPx\text{-}Se^- + H^+ + GSSG} \quad (3)$$

$$\mathrm{GSSG + NADPH + H^+ \xrightarrow{GR} 2GSH + NADP^+} \quad (4)$$

Address correspondence to: Garry R. Buettner, Ph.D., Free Radical Research Institute, EMRB 68, The University of Iowa, Iowa City, IA 52242-1101, USA; Tel: (319) 335-6749; Fax: (319) 335-8049, E-Mail: garry-buettner@uiowa.edu.

PhGPx has been detected in cytoplasm and mitochondria, as well as in plasma and nuclear membranes [11]. There are two forms of PhGPx: a mitochondrial form (L-PhGPx), and a nonmitochondrial form (S-PhGPx). L-PhGPx, containing a 27 amino acid leader sequence [12], is located in the intermembrane space of the mitochondria. Higher activities have been observed at the contact sites of the inner- and outer-mitochondrial membranes [13]. S-PhGPx is present in the cytosol, where it is associated with plasma, nuclear, or other organelle membranes [9]. PhGPx appears to be effective in preventing cell death caused by reactive oxidative species (ROS) [14–16]. It is a key enzyme in the defense against oxidative damage of biomembranes.

A goal of this research was to explore the role of PhGPx in $^1O_2$-induced cell damage. We used Photofrin, a photosensitizer used in photodynamic therapy (PDT) for cancer treatment, as a tool to introduce $^1O_2$ into cellular membranes. Singlet oxygen reacts with unsaturated lipids forming LOOHs [17]. We hypothesized that PhGPx would reduce $^1O_2$-induced cytotoxicity by removing the LOOHs formed in membranes. Human breast carcinoma cells (MCF-7) that overexpress human PhGPx were established as a model system. Overexpression of PhGPx significantly enhanced the removal of $^1O_2$-induced cellular LOOH and suppressed free radical-mediated lipid peroxidation. Cell survival correlated directly with PhGPx activity. Our results indicate that lipid hydroperoxides are key mediators in $^1O_2$-induced cell injury, and that PhGPx is remarkably effective in preventing cell death from hydroperoxide-mediated oxidation. Thus, PhGPx could protect against the oxidative stress induced by some xenobiotics or confer resistance to medical treatments that have lipid peroxidation involved in their mode of action.

EXPERIMENTAL PROCEDURES

Reagents

The primary antibody against rat PhGPx was a generous gift from Dr. Albert W. Girotti (Medical College of Wisconsin). Horseradish peroxidase conjugated to goat anti-rabbit IgG was purchased from Boehringer Mannheim Corp. (Indianapolis, IN, USA). L-α-phosphatidylcholine type III/S, lipoxidase, type IV, sodium deoxycholate, glutathione (GSH), glutathione reductase (GR), NADPH, Triton X-100 (peroxide-free), sodium azide, sodium selenite, and 5,5-dimethyl-pyrroline-1-oxide (DMPO) were obtained from Sigma (St. Louis, MO, USA). DMPO was purified with activated charcoal/benzene, and then prepared as a 1.0 M aqueous stock solution [18,19]. LipofectAMINE, minimum essential medium (MEM), fetal bovine serum (FBS), and Geneticin (G418) were purchased from GIBCO (Grand Island, NY, USA). Photofrin® (porfimer sodium) was a gift from QLT Phototherapeutics, Inc. (Vancouver, BC, Canada). A stock solution was made in 5% dextrose (pH 7.4), filtered (0.2 μm Nalgene filter, Nalgene Co., Rochester, NY, USA) and frozen at −20°C.

Plasmid construction

The pBluescript plasmid containing the human mitochondrial form PhGPx cDNA was kindly provided by Dr. Rugao Liu (Howard Hughes Institute, Roseville, MN, USA). It was prepared by RT-PCR. The 800 base pair fragment containing the L-PhGPx cDNA was digested and ligated into the pcDNA3.1(−) mammalian expression vector (Invitrogen Co., San Diego, CA, USA) between the EcoRI and HindIII restriction enzyme sites with a 5′ to 3′ orientation. The DNA insert was sequenced bidirectionally using the Sanger-based dideoxy sequencing strategy that involves the incorporation of fluorescence dye-labeled terminators into the sequencing reaction products.

Cell culture and transfection

MCF-7 cells (American Type Culture Collection) were cultured in MEM containing 10% fetal bovine serum (FBS), 1% nonessential amino acids, 30 nM sodium selenite, at 37°C, 5% CO_2. Cells (5×10^4) were seeded into 6 well plates 24 h before transfection. The expression plasmid vector pcDNA3.1(−) and the plasmid containing human PhGPx cDNA were transfected into MCF-7 cells using LipofectAMINE reagent according to the instructions provided by the manufacturer (LifeTech Inc., Rockville, MD, USA). Briefly, 72 h after transfection, cells were trypsinized and seeded at low density into 35 mm culture dishes in MEM containing 10% FBS with 1 mg/ml G418. Two weeks after transfection, the surviving clones were isolated, transferred to 24 well plates, and grown in MEM with 10% FBS and 350 μg/ml G418. Stably transfected cell lines, P-1, P-2, P-3, and P-4 with different overexpression levels of PhGPx, as well as the cells transfected with the vector only, were maintained in MEM with 350 μg/ml G418 and 30 nM sodium selenite. Two days before an experiment, G418 was removed.

RT-PCR for PhGPx

Total cellular RNA was isolated from transfected and nontransfected cells using Qiagen RNeasy Kit (QIAGEN Inc., Valencia, CA, USA) and quantified by UV spectrophotometer at 260 nm. Total RNA (5 μg) was converted

into cDNA by priming in a reaction solution containing 2 μl oligo (dT) primer (20 μM), 2 μl of dNTP mixture (10 mM each of dATP, dGTP, dCTP, dTTP), 2 μl of dithiothreitol (DTT) (100 mM), 1 μl of RNase inhibitor (RNasin) (40 units/μl), 2 μl of Moloney-Murine Leukemia Virus (MMLV) reverse transcriptase (200 units/μl), 8 μl of 5$\times$ first strand buffer (50 mM Tris-HCl, pH 8.3, 3 mM $MgCl_2$, 75 mM KCl). The mixture was incubated for 1 h at 42°C to synthesize cDNA, and then for 15 min at 70°C to inactivate the enzyme. The solution containing the synthesized cDNA was diluted to 100 μl with nanopure water and stored at $-$20°C.

PCR primers were designed based on the human PhGPx cDNA sequence [20]. The sequences of oligonucleotide primers were as follows: L-PhGPx sense, 5′-CTTTGCCGCCTACTGAAG-3′; S-PhGPx sense, 5′-TCCATGCACGAGTTTCC-3′; antisense, 5′-GATCCGCAAACCACACTC-3′. The PCR products of L-PhGPx and S-PhGPx were 275 bp long and 174 bp long, respectively. PCR was carried out in a 50 μl mixture containing 5 μl 10$\times$ PCR buffer, 1 μl 10 mM dNTP, 1 μl Taq DNA polymerase (5 units/μl), 5 μl of cDNA, 1 μl of sense and antisense primer mixture (20 μM each), 1 μl of antisense primer, and 37 μl nanopure water. PCR was conducted in a thermal cycler (Perkin Elmer GeneAmp PCR System 2400, Norwalk, CT, USA). After 3 min of denaturation at 94°C, the amplification was carried out with 30 cycles. The thermal cycling profile consists of denaturation at 94°C for 1 min, annealing at 55°C for 1 min, and extension at 72°C for 1:30 min, followed by a final extension at 72°C for 7 min. The PCR products (30 μl) were resolved in a 1.5% agarose gel with ethidium bromide staining. Positive controls: pure L-PhGPx cDNA was amplified in PCR mixture; Negative controls: the PCR mixture was amplified without template cDNA.

Western blot

Cells were grown to 80% confluence in 100 mm dishes, washed twice with phosphate-buffered saline (PBS), and harvested by scraping. The cell pellet was sonicated and protein concentration was determined using the BioRad Protein Assay kit (Bio-Rad Laboratories, Hercules, CA, USA). Total denatured protein (200 μg) was resolved on a 12.5% SDS-PAGE and electrotransferred onto a nitrocellulose membrane (Schleicher and Schuell, Keene, NH, USA). The membrane was incubated with rabbit anti-rat PhGPx polyclonal antibody (1:100), followed by incubation with horseradish peroxidase conjugated to goat anti-rabbit IgG (1:5000). Detection by the chemiluminescence reaction was carried out for 1 min using the ECL kit (Amersham Pharmacia Biotech, Piscataway, NJ, USA), followed by exposure to Kodak x-ray film. Densitometry analysis was carried out using the AlphaImager 2000 program (Alpha Innotech, San Leandro, CA, USA).

Northern blot

Total cellular RNA was isolated from cells using Qiagen RNeasy Kit (QIAGEN Inc.) and quantified by a UV spectrophotometer at 260 nm. Total cellular RNA (10 μg) was denatured, fractionated on a 1.5% RNA gel, and transferred onto a nylon membrane (Boehringer Mannheim). The membrane was hybridized in the buffer with digoxigenin labeled cDNA probe for PhGPx overnight at 68°C. The hybridized bands were detected with an anti-DIG alkaline phosphatase conjugated antibody, followed by exposure to Kodak x-ray film.

Activity assay for PhGPx

The activity was measured by a coupled enzymatic assay using GSH, glutathione reductase (GR), phosphatidylcholine hydroperoxides (PCOOH), and NADPH with some modification [11]. The assay mixture contained (in 1 ml) the following (final concentrations): 0.1 M Tris-HCl (pH 8.0), 2 mM disodium ethylenediamine tetraacetate (EDTA), 1.5 mM NaN_3, 0.1% Triton X-100 (peroxide free), 3 mM GSH, 1.5 U/ml GR, and an aliquot of cell homogenate (1 mg total cell protein). This mixture was incubated at 37°C for 8 min, then 0.2 mM NADPH was added and incubated for 8 min to allow the enzyme and GSSG to be converted to the reduced form. The nonspecific NADPH oxidation rate was recorded for 4 min at 340 nm; then the enzyme reaction was started by the addition of PCOOH (10–30 μM). The rate of specific NADPH oxidation was recorded every 20 s for 4 min at 340 nm using a Beckman DU-70 spectrophotometer. The activity was calculated by subtracting the nonspecific NADPH oxidation rate from the observed NADPH oxidation rate after the substrate addition. The specific activity is expressed as milliunits per milligram total cell protein; one unit of enzyme activity catalyzes the oxidation of 1 μM of NADPH per minute.

The substrate (PCOOH) was prepared by enzymatic hydroperoxidation of phosphatidylcholine using soybean lipoxidase type IV [11]. A mixture of 22 ml of 0.2 M Tris-HCl pH 8.8, containing 3 mM sodium deoxycholate and 0.3 mM phosphatidylcholine was stirred continuously at room temperature. The reaction was started by adding 0.7 mg of soybean lipoxidase type IV for 30 min. The mixture was loaded onto a Sep-Pak Plus C_{18} cartridge (Part No. WAT 020515, Waters, Milford, MA, USA) that had been equilibrated with 4 ml methanol and 40 ml water. After washing with 220 ml of water, PCOOH was eluted with 2 ml methanol. The final con-

centration of PCOOH in methanol was typically about 2 mM. The concentration of PCOOH was determined spectrophotometrically using a 100-fold dilution in methanol and $\varepsilon_{234} = 25{,}000\ M^{-1}cm^{-1}$ [21]. The substrate is stable at −20°C for at least 1 month. Because this assay is not specific for PCOOH, as other oxidized lipid products can result in conjugated diene formation, we used one batch for all experiments insuring that the [PCOOH] was always the same.

Photosensitization with Photofrin

Cells were incubated with 6 μg/ml Photofrin in serum-containing medium for 24 h. After being washed with PBS three times, cells were illuminated with visible light (5 J/m^2s) on a light box for different time points [22]. Cells were then incubated in complete medium at 37°C for 6 h in the dark. After this incubation, cells were subjected to assays. Cells treated with Photofrin but no light exposure were used as controls.

LOOH assay

The extent of lipid peroxidation after photosensitization was determined as lipid hydroperoxides using a Lipid Hydroperoxide Kit (Cayman, Ann Arbor, MI, USA). Briefly, cells were seeded into 100 mm dishes. Cell membranes were extracted using chloroform:methanol (2:1, *v/v*). Ferrous iron was added to the chloroform layer and formation of ferric thiocyanate ion was measured at 500 nm on a Beckman DU-70 spectrophotometer. 13-Hydroperoxy octadecadienoic acid (13-HpODE) was used as the standard.

EPR spin trapping combined with Folch extraction

Lipid-derived radical formation in cells was determined using EPR spin trapping [23]. Cells (1×10^6) were seeded into 100 mm dishes 24 h before the experiment. After treatment with Photofrin and light, cells were washed (2×) with metal-free PBS [24] and then incubated for 5 min with 150 mM DMPO and 100 μM $Fe(NH_4)_2(SO_4)_2 \cdot 6H_2O$ in 5 ml metal-free PBS buffer. Control cells were incubated with Photofrin but not exposed to light. Cells were then scraped off; the cells and the PBS mixture were extracted using 15 ml chloroform: methanol (2:1, *v/v*). After phase separation overnight, the lower chloroform layer was collected and dried completely under argon. The extracted lipid products were resuspended in 500 μl degassed ethyl acetate and immediately transferred into an EPR flat cell for EPR measurement. EPR signal intensity was recorded on a Bruker ESP-300 spectrometer (Billerica, MA, USA) equipped with a TM_{110} cavity operating at 9.76 GHz with modulation frequency 100 kHz, modulation amplitude 1.0 G, and microwave power 40 mW. Each spectrum represents the signal-averaged result of 45 scans of the DMPO/lipid-derived radical adduct. All experiments were performed at room temperature.

Membrane permeability

Cells (1×10^5) were seeded into 35 mm dishes 24 h before Photofrin photosensitization. After $^1O_2$-stress, cells were incubated 6 h to allow the enzymatic repair and then cells were washed and trypsinized. Cells were stained with 0.2% trypan blue.

Flow cytometer

Cell death was assayed via flow cytometry (FACScan) using Annexin V and propidium iodide (PI) staining. After exposure to singlet oxygen, cells were washed and trypsinized. Cells were then stained with 2 μg/ml Annexin V in Annexin V binding buffer (Palo Alto, CA, USA) for apoptosis measurement or stained with 5 μg/ml PI for detection of necrosis.

Cytotoxicity

A clonogenic survival assay was used to measure singlet oxygen-induced cytotoxicity. Cells (3×10^5) were plated in 60 mm dishes. After photosensitization, cells were trypsinized and seeded into 6 well plates. Colonies containing more than 50 cells were counted after 2 weeks.

Statistics

ANOVA Tukey test was used for the comparison of different groups. The null hypothesis was rejected at the 0.05 level of significance. Linear regression analyses were performed with the Microsoft Excel program (Excel 97 SR-1).

RESULTS

Overexpression of PhGPx in MCF-7 cells

To examine the role of PhGPx in the protection of cells against the oxidative stress induced by singlet oxygen, we stably transfected MCF-7 cells with human PhGPx cDNA. The presence of PhGPx was assessed using RT-PCR, western and northern blotting analyses, and PhGPx activity assay. Four clones (P-1, P-2, P-3, P-4) with various expression levels were selected for study. To confirm that L-PhGPx is overexpressed in the

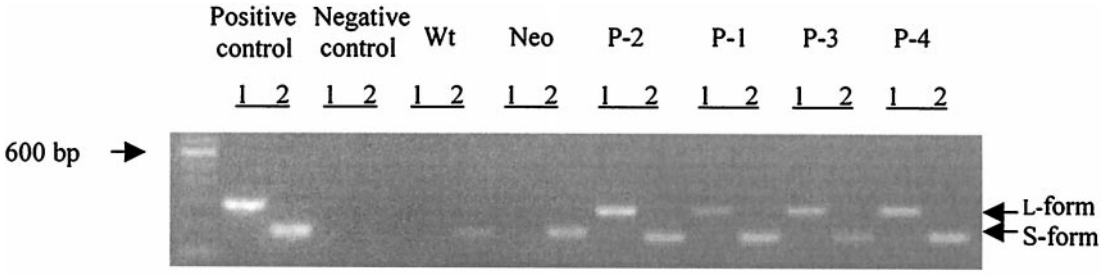

Fig. 1. Detection of L-PhGPx and S-PhGPx in MCF-7 cells using RT-PCR. PhGPx cDNA was prepared by the reaction of total cellular RNA (5 μg) with oligo (dT) using RT. The resulting cDNA was amplified in a 50 μl PCR mixture for 30 thermal cycles. The PCR products (30 μl) were separated in a 1.5% agarose gel staining with ethidium bromide. Positive control: the pure L-PhGPx cDNA was amplified in PCR mixture; Negative control: the PCR mixture was amplified without template cDNA; Lanes 1: with the L-form primer; Lanes 2: with the S-form primer. Data are representative of three independent experiments.

transfected cells the L- and S-forms of PhGPx were determined using RT-PCR (Fig. 1). The RT-PCR data provide only qualitative but not quantitative information due to the lack of an internal standard. S-PhGPx was found in all the cells. L-PhGPx was found only in the PhGPx transfected cells.

Figure 2 shows the immunoreactive protein (panel A), and steady-state mRNA levels (panel B) of PhGPx in the cells used in this study. Both the parental cells (Wt) and the vector only control (Neo) had detectable levels of PhGPx protein, but mRNA levels were below the limit of detection. This inconsistency could come from an instability of endogenous PhGPx mRNA. P-1 and P-2 cells had low and medium expression of PhGPx, while P-3 and P-4 cells strongly expressed PhGPx at both protein and mRNA levels. Total PhGPx activity increased 3- to 4-fold in P-1 and P-2 cells, and increased 7- to 8-fold in P-3 and P-4 cells, compared to the Wt and Neo controls (Fig. 3A). There was a direct linear correlation between PhGPx protein and activity levels ($r = 0.99$; Fig. 3B). Transfection of PhGPx did not result in significant changes in the activity of the other cellular antioxidants (CuZnSOD, MnSOD, cGPx, catalase, GR, and GSH data not shown). The levels of these enzymes were the same as reported by Yan et al. for MCF-7 cells [25]. Thus, increase of PhGPx activity appears not to influence the profile of the other antioxidant enzymes in these cells.

PhGPx decreases cellular lipid hydroperoxide levels induced by PDT

Singlet oxygen ($^1O_2$) produced by PDT reacts with the polyunsaturated fatty acids (PUFAs) in cell membranes forming LOOHs [22,23]. We hypothesized that cells with higher PhGPx levels would more rapidly remove these LOOHs. To test this hypothesis, cells were incubated with Photofrin and then illuminated to seed

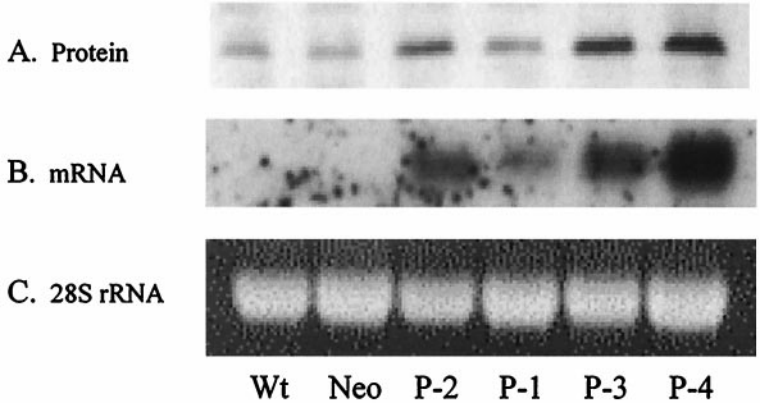

Fig. 2. MCF-7 cells stably transfected with human PhGPx cDNA have increased levels of PhGPx mRNA and protein. (A) Western blot. Protein (200 μg) from each cell line was separated on a 12.5% SDS polyacrylamide gel. An increased expression of PhGPx is observed in the ≈20 kDa band in the four transfected cell lines (P-1, P-2, P-3, and P-4). The Neo cells (vector only) had the similar expression level as the Wt (wild type). (B) Northern blot. Total RNA (10 μg) was separated on a 1.5% RNA agarose gel. A band corresponding to PhGPx mRNA was found in the transfected cells. No bands were detectable in Wt and Neo cells. (C) Loading control. The 28S rRNA was used as the loading control for northern blot. Data are representative of three independent experiments.

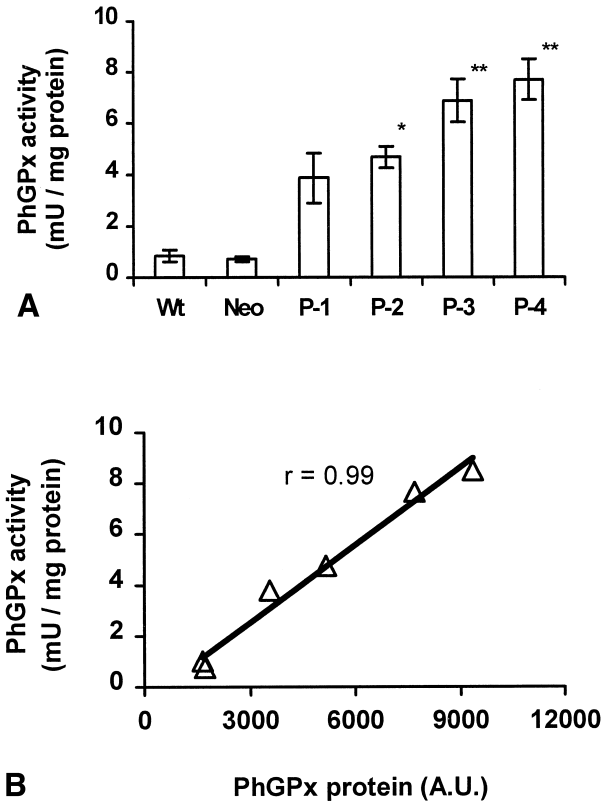

Fig. 3. MCF-7 cells stably transfected with human PhGPx cDNA have increased PhGPx activity. (A) Cellular PhGPx activity was measured by the coupled enzymatic assay at 340 nm. The phosphatidylcholine hydroperoxide (20 μM) was used as the substrate. One unit of PhGPx activity is defined as the amount of protein required to oxidize 1 μM of NADPH per minute [26–28]. Results are mean ± SE, $n = 3$, $^{*}p < .05$; $^{**}p < .001$ compared to Wt. (B) Data are derived from Figs. 2A (densitometry analysis) and 3A.

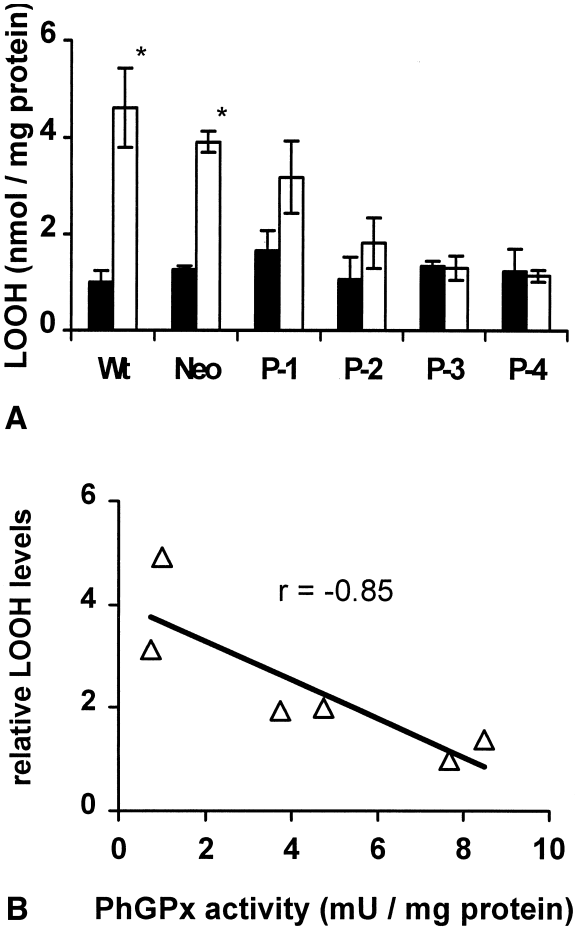

Fig. 4. PhGPx removes LOOHs formed by exposure of MCF-7 cells to $^1O_2$. (A) Cells were pretreated with 6 μg/ml Photofrin for 24 h in full media. After 5 min light exposure, cells were incubated for 6 h in the dark. LOOH levels were assessed using the Cayman Lipid Hydroperoxide Kit. (Data are mean ± SE, $n = 3$, $^{*}p < .05$ compared to the nonlight exposure control). Solid bars: control, cells exposed to Photofrin, but no light. Open bars: cells treated with Photofrin and light. (B) Removal of LOOHs correlates with PhGPx activity; data are derived from Figs. 3A and 4A (Sample data from Fig. 4A were divided by the corresponding controls). The same trend is observed if the control values are subtracted from the corresponding sample data and plotted versus PhGPx activity.

LOOHs into cell membranes. Immediately after light exposure LOOH levels increased from a background level of approximately 1 nmol/mg protein to 5 nmol/mg protein in all six cell lines. There was no statistical difference in the levels of LOOHs between Wt, Neo, and the transfected cells (data not shown). This result indicated that increased PhGPx at the level we were able to obtain did not influence the formation of LOOHs from singlet oxygen.

When the six cell lines were incubated in the dark after light exposure to allow for repair, significant differences in LOOH levels were observed (Fig. 4A). After 6 h, Wt and Neo cells still had 4- to 5-fold more LOOHs compared to their nonilluminated controls. The two clones with low to medium PhGPx levels (P-1, P-2) had 2- to 3-fold more LOOHs compared to their controls. However, the two clones having the highest PhGPx activity (P-3, P-4) fully repaired the $^1O_2$-induced LOOHs, as only background levels of LOOHs were observed in these cells. The levels of LOOHs were inversely correlated with PhGPx activity ($r = -0.85$; Fig. 4B).

PhGPx removes an initiator needed for free radical chain reactions

In the presence of trace amounts of ferrous iron, LOOHs serve as initiators for free radical chain reactions, which can lead to cell death [29,30]. To test our hypothesis that PhGPx will decrease lipid radical chain reactions, we examined lipid-derived radical formation using EPR spin trapping. EPR spin trapping has been demonstrated to be an effective method to

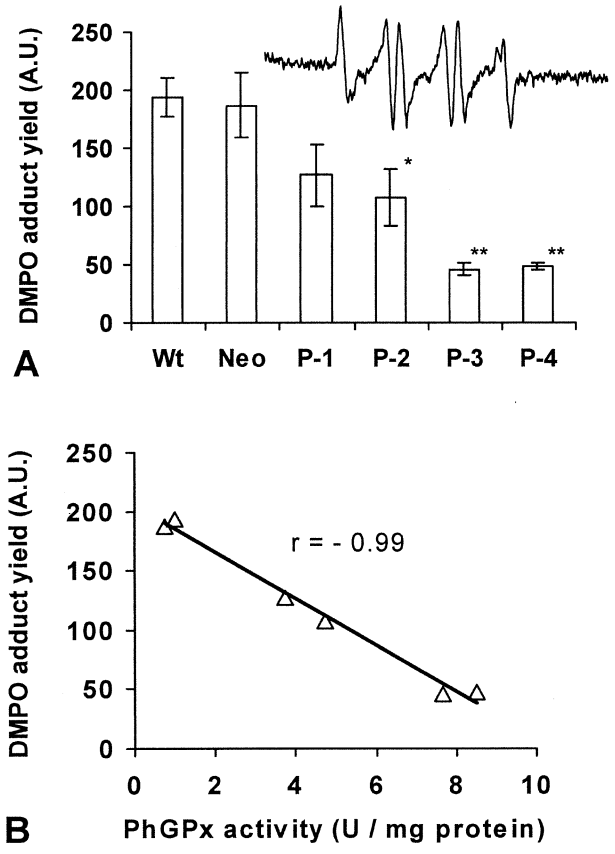

Fig. 5. PhGPx inhibits $^1O_2$-induced lipid-derived radical generation. (A) Cells were pretreated with 6 μg/ml Photofrin for 24 h in full media. After 5 min light exposure, cells were incubated for 6 h in the dark. Radical formation was then assessed using EPR spin trapping. Each spectrum represents the signal-averaged result of 45 scans. The height of the low-field line of the DMPO/lipid-derived radical adduct was used as a measure of radical yield. Inset: An example X-band EPR spectrum of the DMPO adduct (a^N = 15.2 G, a^H = 10.2 G in ethyl acetate) formed from MCF-7 cells. Control cells were incubated with Photofrin but not exposed to light. The yield of DMPO adduct in the control samples was below the limit of detection (data not shown). (Mean ± SE, $n = 3$, $*p < .05$, $**p < .005$ compared to Wt). (B) Lipid radical formation correlates inversely with PhGPx activity. Data are derived from Figs. 3A and 5A.

detect lipid radicals formed in cells [31,32]. LOOHs were seeded into cells by exposure to $^1O_2$. After 6 h incubation in the dark, the spin trap DMPO was added followed by ferrous iron to initiate the radical-mediated lipid peroxidation. The lipid-derived spin adducts were separated from the reaction mixture by Folch extraction (chloroform:methanol) as described by Qian et al. [23]. Lipid-derived radical adducts of DMPO (a^N = 15.2 G, a^H = 10.2 G) were observed by EPR (Fig. 5A). Cells with low PhGPx activity produced high spin adduct signal, while cells with high levels of PhGPx activity resulted in low levels of spin adduct signal. A strong inverse correlation ($r = -0.99$) was found between the amount of DMPO spin adduct formed and the PhGPx activity (Fig. 5B).

PhGPx protects against PDT-induced membrane damage

PDT introduces LOOHs into cellular membranes due to the formation of singlet oxygen. LOOH formation has been suggested to cause the disruption of cell membranes [33]. Because PhGPx removes LOOHs formed in cells, we hypothesized that cells with higher PhGPx activity would be better able to maintain membrane integrity upon exposure to $^1O_2$. To test this hypothesis we examined trypan blue dye exclusion from cells after photosensitization. Membrane integrity was preserved in cells that expressed higher levels of PhGPx; P-3 and P-4 cells were up to four times more resistant than Wt and Neo (at 10 min; Fig. 6A). Membrane integrity, expressed as percent of dye exclusion, correlated directly with the PhGPx activity ($r = 0.89$; Fig. 6B).

PhGPx prevents PDT-induced cell death

To further examine cell death from PDT toxicity in our model system, we used flow cytometric techniques. After cells were stressed with Photofrin and a 10 min light exposure, they were allowed to recover for 6 h in the dark, then cell death was analyzed via a flow cytometer using Annexin V and propidium iodide (PI) staining. Annexin V marks phosphatidylserine on the cell surface and serves as an indicator of apoptosis. As expected, no apoptosis was detected (data not shown), which is consistent with previous reports that MCF-7 cells are resistant to apoptosis [34,35]. However, the changes observed in the patterns for PI staining clearly demonstrated that singlet oxygen induces necrotic cell death (Fig. 7). For the Neo cells, the percentage of cells that gated PI-positive increased from 21% before $^1O_2$ exposure to 94% after exposure, compare Fig. 7A to 7B. However, this same treatment of P-3 cells resulted in a change in the PI positive cells from 22 to 65%, compare Fig. 7C to 7D. These data suggest that overexpression of PhGPx can protect cells from PDT-induced necrotic death.

PhGPx decreases PDT-induced cytotoxicity

Disruption of the cell membrane by LOOHs can lead to cytotoxicity. To examine whether removal of LOOHs modulates the cytotoxicity of singlet oxygen exposure, we performed clonogenic survival assays. As seen in Fig. 8A, PhGPx greatly enhances clonogenic survival. At 10 min of light exposure P-4 cells exhibited a 10-fold higher clonogenic survival than Wt and Neo cells. Clonogenic survival had a strong direct correlation with PhGPx activity ($r = 0.94$; Fig. 8B). These results combined with the above dye exclusion and flow cytometric assays

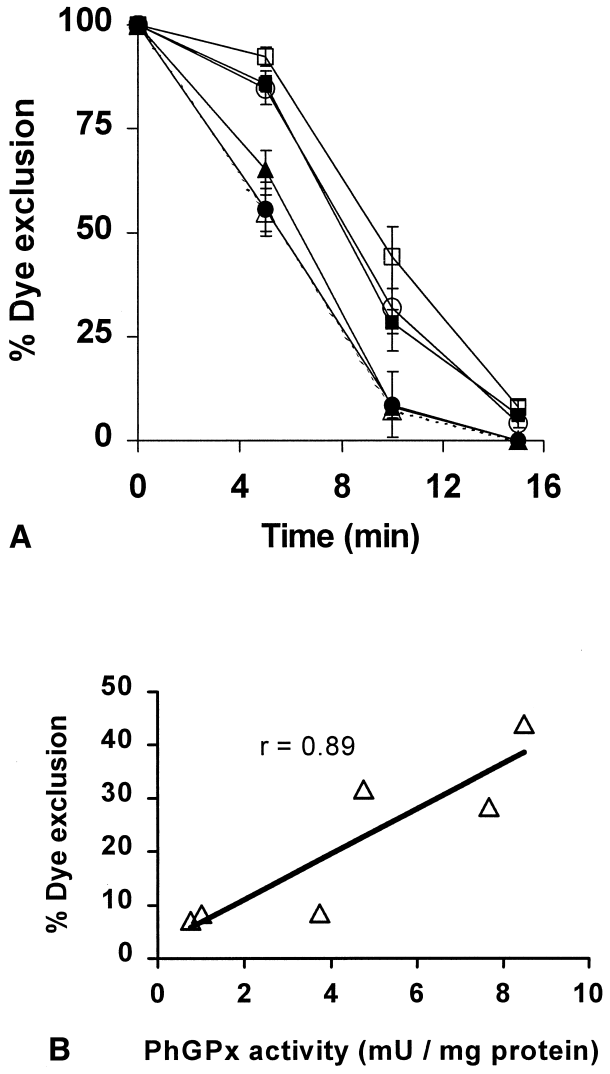

Fig. 6. PhGPx blunts $^1O_2$-induced membrane permeability changes in MCF-7 cells. (A) Cell membrane permeability was assayed by trypan blue dye exclusion. Cells were incubated with Photofrin 6 μg/ml for 24 h, and then irradiated with visible light (0 to 15 min). After light exposure, cells were incubated 6 h in the dark at 37°C. Cells were then trypsinized and assayed for viability. Symbols: ▲ = Wt; △ = Neo; ● = P-1; ○ = P-2; ■ = P-3; □ = P-4. (Data are mean ± SE, $n = 3$). (B) Cell viability at 10 min correlates directly with PhGPx activity. Data are derived from Figs. 3A and 6A.

indicate that enhanced levels of PhGPx can lead to cell resistance to singlet oxygen-induced oxidative damage.

DISCUSSION

Lipids are a major target for oxidative damage in cells. Lipid hydroperoxides are key intermediates in the lipid peroxidation process serving as initiators for free radical chain reactions. The enzymatic repair of these LOOHs is critical for cells to avoid potential lethal damage. There appear to be at least four important enzyme systems (cGPx, GST, non-Se-GPx [36], and PhGPx) that can detoxify LOOHs and thereby reduce or prevent hydroperoxide-mediated cell damage. PhGPx is able to reduce directly phospholipid hydroperoxides, that is, it detoxifies LOOHs inside the cell membrane. Thus, PhGPx could play an important role in protecting cells from the effects of lipid peroxidation [6,15].

To examine the importance of PhGPx in the protection of cells from the damaging effects of LOOHs we developed MCF-7 cells that overexpress human PhGPx. MCF-7 is a tumor cell line that has very low levels of MnSOD and cGPx compared to normal counterparts [25,37]; it also has a low level of PhGPx protein [38]. Our western blot, northern blot, and PhGPx activity assays showed that MCF-7 cells can express higher levels of PhGPx when stably transfected (Fig. 2). The PhGPx activity observed in the various MCF-7 cell lines studied showed a high direct linear correlation with PhGPx protein (Fig. 3). The results from the RT-PCR (Fig. 1) show that the increased mRNA and protein levels of PhGPx in the transfected cells result primarily from the L-form.

Singlet oxygen is an ideal tool to introduce LOOHs into cell membranes. PhGPx did not appear to influence the formation of these LOOHs but rather removed them. After 6 h, all LOOHs formed by singlet oxygen were removed in the transfected cells, whereas cells with low expression still had significant levels of LOOHs remaining at this time; the removal of LOOHs correlated directly with PhGPx activity (Fig. 4). Removal of LOOHs by PhGPx prevented potential free radical formation as observed by EPR spin trapping (Fig. 5).

Because lipid peroxidation can be detrimental to cells, we hypothesized that increasing PhGPx activity would increase the resistance of cells to oxidative stress. Formation of LOOHs and the subsequent lipid peroxidation reactions can interrupt the integrity of cell membranes. Indeed, PhGPx was able to maintain membrane integrity upon exposure to singlet oxygen (Fig. 6). Cell survival, as assessed by clonogenic assay and flow cytometry, was also significantly increased in cells with high levels of PhGPx activity (Figs. 7 and 8).

Transfection of PhGPx did not change the intracellular antioxidant profile (cGPx, catalase, MnSOD, CuZn-SOD, GR activities, and total cellular GSH levels), data not shown. Thus, the removal of LOOHs and the increase in cell survival in response to $^1O_2$ is due to PhGPx overexpression.

Previous studies on the role of cGPx and PhGPx in protecting cells against $^1O_2$-mediated phototoxicity used selenium depletion as a tool to modulate PhGPx activity [39]. Depletion as well as supplementation of cell culture media with Se can result in changes in both cGPx and

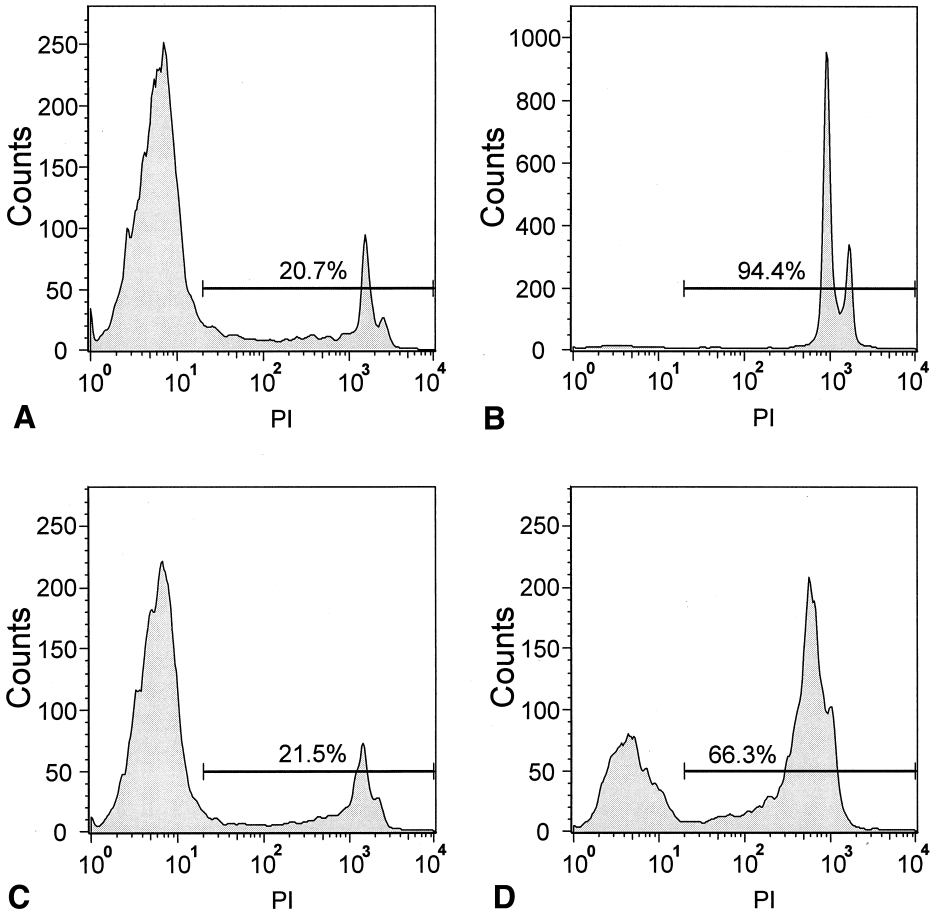

Fig. 7. PhGPx decreases $^1O_2$-induced necrotic death in MCF-7 cells. Flow cytometry analysis of Neo and P-3 cells exposed to $^1O_2$. Cells were incubated with Photofrin (6 μg/ml) for 24 h, followed by irradiation with visible light (10 min). After that, cells were incubated 6 h in the dark at 37°C. Cells were washed and trypsinized, stained with 5 μg/μl PI in MEM. Cells were analyzed by flow cytometry. The percentages shown represent the percent of cells that were PI positive. (A) MCF-7 Neo without light; (B) MCF-7 Neo with light; (C) P-3 cells without light; (D) P-3 cells with light. Data are representative of three independent experiments.

PhGPx activities. The changes upon supplementation were cell line-dependent. An increase in PhGPx afforded protection from the potential toxicity of phospholipid hydroperoxides. Using molecular biology techniques, we were able to achieve different levels of PhGPx activity without changing the activity of other antioxidant enzymes in cells. This allowed us to investigate quantitatively the importance of PhGPx activity in providing protection from toxicity of singlet oxygen. This quantitative approach has made it possible for the first time to demonstrate the strong correlation between PhGPx activity and various biological endpoints.

PhGPx activity correlates inversely with intracellular levels of lipid hydroperoxides and potential radical formation upon exposure to singlet oxygen. The importance of the removal of lipid hydroperoxides is supported by the strong direct correlation seen between PhGPx activity and cell survival after an oxidative stress. Taken together, these data support LOOHs as being major mediators in cell injury. PhGPx is a key enzyme in protecting cells from the damaging effects of lipid peroxidation resulting from oxidative stress.

Many xenobiotics, be they drugs for treatment of disease or pollutants from environmental exposure, result in the production of reactive oxygen species. Resistance to such an oxidative stress will depend on the antioxidant capacity of the cells and tissues. Because PhGPx is present only in small amounts in cells, compared to the other antioxidant enzymes, it has been largely overlooked by the scientific community. However, it has been estimated that under physiological conditions the rate of removal of LOOHs through PhGPx is about four orders of magnitude greater than through the cGPx and PLA_2 system [10]. In addition, a dietary study of selenium deficiency in mice found that PhGPx activity was more slowly depleted by Se deficiency than cGPx [40]. Our findings that PhGPx activity strongly correlated with various biological endpoints support the importance of

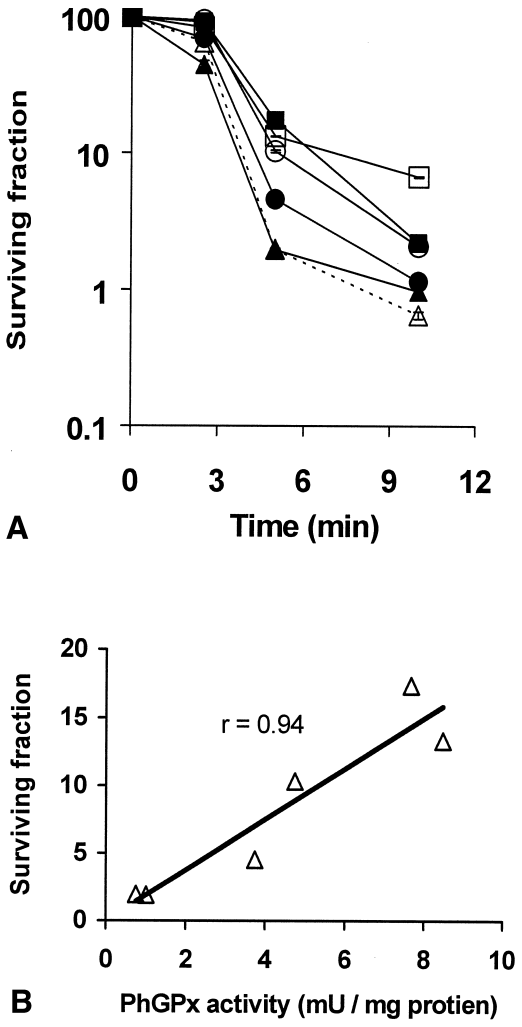

Fig. 8. PhGPx protects against $^1O_2$-induced cytotoxicity in MCF-7 cells. (A) Cell cytotoxicity was measured by clonogenic assay. Cells were incubated with Photofrin 6 μg/ml for 24 h, and then irradiated with visible light (0 to 10 min). After light exposure, cells were incubated 6 h in the dark at 37°C and then seeded into 6 well plates and incubated for 2 weeks to allow colony formation. Surviving fraction is expressed as: ([colonies formed/cells seeded $\times$ plate efficiency] $\times$ 100%). Symbols: ▲ = Wt; △ = Neo; ● = P-1; ○ = P-2; ■ = P-3; □ = P-4. (Mean $\pm$ SE, $n = 3$; the error bars are smaller than the symbols). (B) Cell viability at 10 min correlates directly with PhGPx activity. Data are derived from Figs. 3A and 8A.

PhGPx as an antioxidant enzyme. The ability of PhGPx to remove LOOHs in situ could confer resistance of cells and tissues to oxidative stress that results in the formation of LOOHs. This could be an advantage or disadvantage, depending on the situation. It would be a disadvantage if PhGPx affords cells and tissues (e.g., tumor) to be resistant to the oxidative stress induced by treatments such as PDT. On the other hand, PhGPx could aid in the resistance of cells to oxidative stress due to xenobiotic exposure; this property could protect normal tissue during certain disease treatments.

Acknowledgements — This work was supported by National Institutes of Health Grants CA66081, CA73612 and CA81090. We thank Dr. Rugao Liu for providing the human PhGPx cDNA, and Dr. Albert W. Girotti for the kind gift of PhGPx primary antibody and the pure PhGPx protein as well as his advice on assays for PhGPx. We thank Dr. Hannah Zhang for helpful discussions and Mr. Justin Fishbaugh for his help in the flow cytometric analysis.

REFERENCES

[1] Berliner, J. A.; Heinecke, J. W. The role of oxidized lipoproteins in atherogenesis. *Free Radic. Biol. Med.* **20:**707–727; 1996.
[2] Halliwell, B.; Gutteridge, J. M. C. In: *Free radicals in biology and medicine.* Oxford, UK: Oxford University Press; 1989:188–266.
[3] Witztum, J. L.; Steinberg, D. Role of oxidized low density lipoprotein in atherogenesis. *J. Clin. Invest.* **88:**1785–1792; 1991.
[4] Pradhan, D.; Weiser, M.; Lumley-Sapanski, K.; Frazier, D.; Kemper, S.; Williamson, P.; Schlegel, R. A. Peroxidation-induced perturbations of erythrocyte lipid organization. *Biochim. Biophys. Acta* **1023:**398–404; 1990.
[5] Sevanian, A.; Mukkassah-Kelley, S. F.; Montestruque, S. The influence of phospholipase A2 and glutathione peroxidase on the elimination of membrane lipid peroxides. *Biochim. Biophys. Acta* **223:**441–452; 1983.
[6] Thomas, J. P.; Maiorino, M.; Ursini, F.; Girotti, A. W. Protective action of phospholipid hydroperoxide glutathione peroxidase against membrane-damaging lipid peroxidation. In situ reduction of phospholipid and cholesterol hydroperoxides. *J. Biol. Chem.* **265:**454–461; 1990.
[7] Fisher, A. B.; Dodia, C.; Manevich, Y.; Chen, J. W.; Feinstein, S. I. Phospholipid hydroperoxides are substrates for non-selenium glutathione peroxidase. *J. Biol. Chem.* **274:**21326–21334; 1999.
[8] Hurst, R.; Bao, Y.; Jemth, P.; Mannervik, B.; Williamson, G. Phospholipid hydroperoxide glutathione peroxidase activity of human glutathione transferases. *Biochem. J.* **332:**97–100; 1998.
[9] Ursini, F.; Maiorino, M.; Gregolin, C. The selenoenzyme phospholipid hydroperoxide glutathione peroxidase. *Biochim. Biophys. Acta* **839:**62–70; 1985.
[10] Antunes, F.; Salvador, A.; Pinto, R. E. PHGPx and phospholipase A2/GPx: comparative importance on the reduction of hydroperoxides in rat liver mitochondria. *Free Radic. Biol. Med.* **19:**669–677; 1995.
[11] Roveri, A.; Maiorino, M. Enzymatic and immunological measurements of soluble and membrane-bound phospholipid-hydroperoxide glutathione peroxidase. *Methods Enzymol.* **233:**202–212; 1994.
[12] Pushpa-Rekha, T. R.; Burdsall, A. L.; Oleksa, L. M.; Chisolm, G. M.; Driscoll, D. M. Rat phospholipid-hydroperoxide glutathione peroxidase. cDNA cloning and identification of multiple transcription and translation start sites. *J. Biol. Chem.* **270:**26993–26999; 1995.
[13] Godeas, C.; Sandri, G.; Panfili, E. Distribution of phospholipid hydroperoxide glutathione peroxidase (PHGPx) in rat testis mitochondria. *Biochim. Biophys. Acta* **1191:**147–150; 1994.
[14] Imai, H.; Sumi, D.; Sakamoto, H.; Hanamoto, A.; Arai, M.; Chiba, N.; Nakagawa, Y. Overexpression of phospholipid hydroperoxide glutathione peroxidase suppressed cell death due to oxidative damage in rat basophile leukemia cells (RBL-2H3). *Biochem. Biophys. Res. Comm.* **222:**432–438; 1996.
[15] Arai, M.; Imai, H.; Koumura, T.; Yoshida, M.; Emoto, K.; Umeda, M.; Chiba, N.; Nakagawa, Y. Mitochondrial phospholipid hydroperoxide glutathione peroxidase plays a major role in preventing oxidative injury to cells. *J. Biol. Chem.* **274:**4924–4933; 1999.
[16] Nomura, K.; Imai, H.; Koumura, T.; Arai, M.; Nakagawa, Y. Mitochondrial phospholipid hydroperoxide glutathione peroxidase suppresses apoptosis mediated by a mitochondrial death pathway. *J Biol. Chem.* **274:**29294–29302; 1999.
[17] Girotti, A. W. Mechanisms of lipid peroxidation. *Free Radic. Biol. Med.* **1:**87–95; 1985.

[18] Kotake, Y.; Reinke, L. A.; Tanigawa, T.; Koshida, H. Determination of the rate of superoxide generation from biological systems by spin trapping: use of rapid oxygen depletion to measure the decay rate of spin adducts. *Free Radic. Biol. Med.* **17:**215–223; 1994.
[19] Buettner, G. R.; Oberley, L. W. Considerations in the spin trapping of superoxide and hydroxyl radical in aqueous systems using 5,5-dimethyl-1-pyrroline-1-oxide. *Biochem. Biophys. Res. Commun.* **83:**69–74; 1978.
[20] Esworthy, R. S.; Doan, K.; Doroshow, J. H.; Chu, F. F. Cloning and sequencing of the cDNA encoding a human testis phospholipid hydroperoxide glutathione peroxidase. *Gene* **144:**317–318; 1994.
[21] Bors, W.; Erben-Russ, M.; Michel, C.; Saran, M. Radical mechanisms in fatty acid and lipid peroxidation. In: Crastes de Paulet, A.; Douste-Blazy, L.; Paoletti, R., eds. *Free radicals, lipoproteins, and membrane lipids.* New York: Plenum Press; 1990:1–16.
[22] Schafer, F. Q.; Buettner, G. R. Singlet oxygen toxicity is cell line-dependent: a study of lipid peroxidation in nine leukemia cell lines. *Photochem. Photobiol.* **70:**858–867; 1999.
[23] Qian, S. Y.; Wang, H. P.; Schafer, F. Q.; Buettner, G. R. EPR detection of lipid-derived radicals from PUFA, LDL, and cell oxidations. *Free Radic. Biol. Med.* **29:**568–579; 2000.
[24] Buettner, G. R. In the absence of catalytic metals ascorbate does not autoxidize at pH 7: ascorbate as a test for catalytic metals. *J. Biochem. Biophys. Methods* **16:**27–40; 1988.
[25] Yan, T.; Jiang, X.; Zhang, H. J.; Li, S.; Oberley, L. W. Use of commercial antibodies for detection of the primary antioxidant enzymes. *Free Radic. Biol. Med.* **25:**688–693; 1998.
[26] Flohe, L. Glutathione peroxidase: enzymology and biological aspects. *Klin. Wochenschr.* **49:**669–683; 1971.
[27] Kosower, N. S.; Kosower, E. M. The glutathione status of cells. *Int. Rev. Cytol.* **54:**109–160; 1978.
[28] Li, S.; Yan, T.; Yang, J. Q.; Oberley, T. D.; Oberley, L. W. The role of cellular glutathione peroxidase redox regulation in the suppression of tumor cell growth by manganese superoxide dismutase. *Cancer Res.* **60:**3927–3939; 2000.
[29] Porter, N. A.; Caldwell, S. E.; Mills, K. A. Mechanisms of free radical oxidation of unsaturated lipids. *Lipids* **30:**277–290; 1995.
[30] Paillous, N.; Ferg-Forgues, S. Interest of photochemical methods for induction of lipid peroxidation. *Biochimie* **76:**355–368; 1994.
[31] Wagner, B. A.; Buettner, G. R.; Burns, C. P. Membrane peroxidative damage enhancement by the ether lipid class of antineoplastic agents. *Cancer Res.* **52:**6045–6051; 1992.
[32] Buettner, G. R.; Kelley, E. E.; Burns, C. P. Membrane lipid free radicals produced from L1210 murine leukemia cells by Photofrin photosensitization: an electron paramagnetic resonance spin trapping study. *Cancer Res.* **53:**3670–3673; 1993.
[33] Girotti, A. W. Lipid hydroperoxide generation, turnover, and effector action in biological systems. *J. Lipid Res.* **39:**1529–1542; 1998.
[34] Janicke, R. U.; Sprengart, M. L.; Wati, M. R.; Porter, A. G. Caspase-3 is required for alpha-fodrin cleavage but dispensable for cleavage of other death substrates in apoptosis. *J. Biol. Chem.* **273:**9357–9360; 1998.
[35] Fisher, A. M. R.; Ferrario, A.; Rucker, N.; Zhang, S.; Gomer, C. J. Photodynamic therapy sensitivity is not altered in human tumor cells after abrogation of p53 function. *Cancer Res.* **39:**331–335; 1999.
[36] Fisher, A. B.; Dodia, C.; Manevich, Y.; Chen, J. W.; Feinstein, S. I. Phospholipid hydroperoxides are substrates for non-selenium glutathione peroxidase. *J. Biol. Chem.* **274:**21326–21334; 1999.
[37] Oberley, L. W.; Buettner, G. R. Role of superoxide dismutase in cancer: a review. *Cancer Res.* **39:**1141–1149; 1979.
[38] Maiorino, M.; Chu, F. F.; Ursini, F.; Davies, K. J. A.; Doroshow, J. H.; Esworthy, R. S. Phospholipid hydroperoxide glutathione peroxidase is the 18-kDa selenoprotein expressed in human tumor cell lines. *J. Biol. Chem.* **266:**7728–7732; 1991.
[39] Lin, F.; Geiger, P. G.; Girotti, A. W. Selenoperoxidase-mediated cytoprotection against merocyanine 540-sensitized photoperoxidation and photokilling of leukemia cells. *Cancer Res.* **52:**5282–5290; 1992.
[40] Weitzel, F.; Ursini, F.; Wendel, A. Phospholipid hydroperoxide glutathione peroxidase in various mouse organs during selenium deficiency and repletion. *Biochim. Biophys. Acta* **1036:**88–94; 1990.

ABBREVIATIONS

cGPx—cytosolic glutathione peroxidase
CuZnSOD—copper-zinc superoxide dismutase
DETAPAC—diethylenetriaminepentaacetic acid
DIG—digoxigenin
DMPO—5,5-dimethyl-pyrroline-1-oxide
EDTA—disodium ethylenediaminetetraacetate
EPR—electron paramagnetic resonance
FBS—fetal bovine serum
GSH—glutathione
GSSG—glutathione disulfide
GST—glutathione S-transferase
GR—glutathione reductase
LOOHs—lipid hydroperoxides
MCF-7—human breast carcinoma cells
MEM—minimum essential medium
MnSOD—manganese superoxide dismutase
PBS—phosphate-buffered saline
PCOOH—phosphatidylcholine hydroperoxide
PCR—polymerase chain reaction
PDT—photodynamic therapy
PhGPx—phospholipid hydroperoxide glutathione peroxidase
PI—propidium iodide
PLA_2—phospholipase A_2
PUFAs—polyunsaturated fatty acids
ROS—reactive oxygen species
RT—reverse transcriptase